

Article

Improvement of the Salinized Soil Properties of Fly Ash by Freeze-Thaw Cycles: An Impact Test Study

Zhuo Cheng¹, Gaohang Cui^{1,*}, Zheng Yang², Haohang Gang¹, Zening Gao¹, Daili Zhang¹ and Chen Xi¹

¹ College of Civil Engineering, Northeast Forestry University, Harbin 150040, China; chengzhuo991205@nefu.edu.cn (Z.C.); ganghaohang@nefu.edu.cn (H.G.); gaozening@nefu.edu.cn (Z.G.); delyazhang@nefu.edu.cn (D.Z.); 1051149676@nefu.edu.cn (C.X.)

² School of Automobile, Chang'an University, Xi'an 710064, China; 2018901545@chd.edu.cn

* Correspondence: cghiem@nefu.edu.cn

Abstract: To explore the mechanism of the microstructural change in salinized soil under freeze-thaw cycles and the strength characteristics of subgrade salinized soil improved by fly ash, an unconfined compressive test, a triaxial shear test, and a scanning electron microscopy test were carried out using salinized soil samples with different fly ash contents along the Suihua to Daqing expressway in China. The results showed that after several freeze-thaw cycles, the unconfined compressive strength, triaxial shear strength, cohesion, and internal friction angle of saline soil showed a decreasing trend. With an increase in the fly ash content, the internal friction angle, cohesion, unconfined compressive strength, and shear strength of the improved saline soil first increased and then decreased. When the fly ash content was 15%, the mechanical indexes, such as cohesion and the internal friction angle, reached the maximum value. Microscopic test results showed that the freeze-thaw cycle will lead to an increase in the proportion of pores and cracks, an increase in the average pore size, and a loosening of the soil structure. The addition of fly ash can fill the soil pores, improve the microstructure of the soil, increase the cohesive force of the soil particles, and improve the overall strength of the soil. Fly ash (15%) can be added to subgrade soil in the process of subgrade construction in the Suihua-Daqing expressway area to improve the shear strength and the resistance to freezing and thawing cycles. These research results are conducive to promoting the comprehensive utilization of fly ash, improving the utilization rate of resources, and promoting sustainable development, thus providing a reference for the design and construction of saline soil roadbed engineering in seasonal frozen areas and the development and construction of saline land belts in seasonal and winter areas.

Keywords: fly ash; saline soil; seasonally frozen area; unconfined compressive strength; shear strength; microscopic pore structure



Citation: Cheng, Z.; Cui, G.; Yang, Z.; Gang, H.; Gao, Z.; Zhang, D.; Xi, C. Improvement of the Salinized Soil Properties of Fly Ash by Freeze-Thaw Cycles: An Impact Test Study. *Sustainability* **2021**, *13*, 2908. <https://doi.org/10.3390/su13052908>

Academic Editor: Dilan J. Robert

Received: 26 January 2021

Accepted: 4 March 2021

Published: 8 March 2021

Publisher's Note: MDPI stays neutral with regard to jurisdictional claims in published maps and institutional affiliations.



Copyright: © 2021 by the authors. Licensee MDPI, Basel, Switzerland. This article is an open access article distributed under the terms and conditions of the Creative Commons Attribution (CC BY) license (<https://creativecommons.org/licenses/by/4.0/>).

1. Introduction

Saline and alkaline soil, as well as the soil following salinization and alkalization, are referred to as saline soil [1,2]. Due to the large amount of salt in pore water, the structural and strength changes of salinized soil in seasonal permafrost regions are more complex than the changes in the strength and structure of saline soil in non-saline soil [3]. When the external temperature, moisture, and other conditions change, the pores inside the saline soil will increase, the soil will soften, or the volume will increase. The mechanical properties of saline soil in seasonal permafrost areas are usually poor. If this material is directly used as a basic filling material, a variety of engineering problems may occur [4], such as road grouting, melting settlement, subgrade settlement, and slope stability reduction. Therefore, to maintain the sustainability of engineering construction in seasonal frozen soil areas and to improve the durability of engineering in these areas, it is of great engineering significance to study the influence of the freeze-thaw cycle on the strength characteristics of saline soil and to improve the properties of saline soil.

Current studies have shown that the unconfined compressive strength of undisturbed soil and improved soil will decrease with the increase in the number of freeze-thaw cycles [5,6]. The cohesion comprehensively reflects various physical and chemical forces, and the internal friction angle reflects the slip or interlocking effect between soil particles [7]. Therefore, these two parameters, cohesion and the internal friction angle, are also widely used in the study of the properties of saline soil after freeze-thaw cycles. Wang et al. [8], Xu et al. [9], and Zhang et al. [10] showed that with the increase in the number of freeze-thaw cycles, both cohesion and the internal friction angle showed a downward trend on the whole, but the internal friction angle may fluctuate in the process of change. The change in the soil engineering properties under freeze-thaw conditions is mainly due to the destruction of the soil structure. Freeze-thaw cycles can change the grain size distribution of soil [11,12] and can also lead to changes in the internal void structure and skeleton of soil [8,13]. Aldaood et al. [14] revealed the effects of water penetration and crack propagation on soil structure through mercury injection and scanning electron microscopy (SEM). Qi et al. [15] studied the shear strength and microstructure of silty clay and loess before and after freeze-thaw cycles through mechanical and SEM tests. They pointed out that the microstructure of soil was an important characteristic for explaining its mechanical properties. Through SEM analysis, Wang et al. [10] provided a quantitative basis for explaining the change mechanism of the mechanical properties of saline soil from a microscopic perspective. Previous studies have shown that the strength of soil is closely related to its microstructure [10,14,15], and the study of the microstructure of soil under freeze-thaw cycles is conducive to the study of the mechanism of the influence of freeze-thaw cycles with respect to the properties of saline soil.

While a great deal of research has been done on the basic properties of salted soil, some achievements have been made in the concrete construction of salted soil areas and the application of modifiers to improve salted soil road performance under freeze-thaw conditions [16–18]. Takeshi et al. [16] used recycled kyanite obtained from gypsum waste as a stabilizing material for soft clay, which improved the durability and strength of saline soil under freeze-thaw cycles. LV et al. [17] used lime, fly ash, and sodium silicate to solidify fine-grained salted sulfate soil, and their study showed that the addition of a curing agent could effectively inhibit the salt-swelling characteristics of salted sulfate soil and improve its strength. Li et al. [18] used fly ash produced by a local power plant to solidify salinized soil and obtain an environmentally friendly, improved, and solidified super-salinized soil. At present, most of the studies on saline soil characteristics and the effect of the application of modifiers on these characteristics have reported on the moisture content of the salt, the modifier dosage, and the influence of various factors on the saline soil strength. However, there is limited research on saline soil that is seasonally frozen (under the effect of the freezing and thawing cycles), especially with respect to the effect and mechanism of action of added modifiers on the quantitative changes in the relevant parameters, microstructure, and strength of the saline soil.

At present, most sections of the Suihua to Daqing expressway (Sui-Da Expressway) of China under planning and construction are saline soil sites, and this area is a seasonal frozen soil area, with a long winter, a large temperature difference between day and night, and long-term temperature below zero degrees Celsius in winter. According to data from the China Meteorological Network, the lowest temperature in Suihua since 2011 reached $-34\text{ }^{\circ}\text{C}$, and the average temperature in January, February, and December has been $-20\text{ }^{\circ}\text{C}$, $-15\text{ }^{\circ}\text{C}$, and $-17\text{ }^{\circ}\text{C}$, respectively. This special environment exposes the local subgrade soil to freeze-thaw cycles over a long period. Such periodic changes will lead to subgrade loosening and will threaten the operation of the road.

Using fly ash to improve the salinized soil subgrade can improve the soil shear strength and stability. Compared with other improvement methods, this approach can reduce the construction cost and accelerate the comprehensive utilization process of fly ash, which has good economic and environmental significance.

In this study, we studied the suitable use of fly ash-modified sulfuric saline soil for roads in cold regions. Fly ash was used as a modifier considering the influence of different freeze-thaw cycles on the saline soil; analysis was conducted on the effect of different dosages of fly ash applied during the freezing and thawing cycle on the unconfined compressive strength and shear strength of the saline soil; the influence of freeze-thaw cycles on the saline soil characteristics was determined; finally, the influence of Image-Pro Plus (IPP) on the soil microstructure was determined using SEM experiments.

We found that the strength characteristics of subgrade salinized soil improved by fly ash, and the shear strength, cohesion, and internal friction angle of soil with 15% fly ash content obtained the highest values. These results provided a reference for the design and construction of saline soil roadbed engineering in seasonal frozen areas and the construction of saline land belts in seasonal and winter areas.

2. Basic Properties of the Test Materials

2.1. Soil Properties

The test soil samples were taken from permafrost soil samples 0.5 m⁻¹ m belowground along the Sui-Da Expressway. The site's surface was exposed, and the surface soil was seriously affected by the salt deposited in the evaporation process. When dry, it was white and shell-like, and there were many macro-microscopic cracks on the surface, and the soil showed obvious characteristics of salinization. According to the Code for Geotechnical Engineering Investigation (GB50021-2001) [19], the soil was a clay silt soil. The particle size distribution was determined by the screening method, as shown in Figure 1. The physical parameters of the soil were analyzed and determined in the laboratory according to Highway Geotechnical Test Rules (JTGE40-2007) [20], as shown in Table 1. The mass ratio of soluble salt ions is shown in Table 2. According to the Geotechnical Engineering Investigation Code (GB50021-2001) [19], the $Cl^- / 2SO_4^{2-}$ of the sample is 0.297, i.e., the soil is sulfate saline soil.

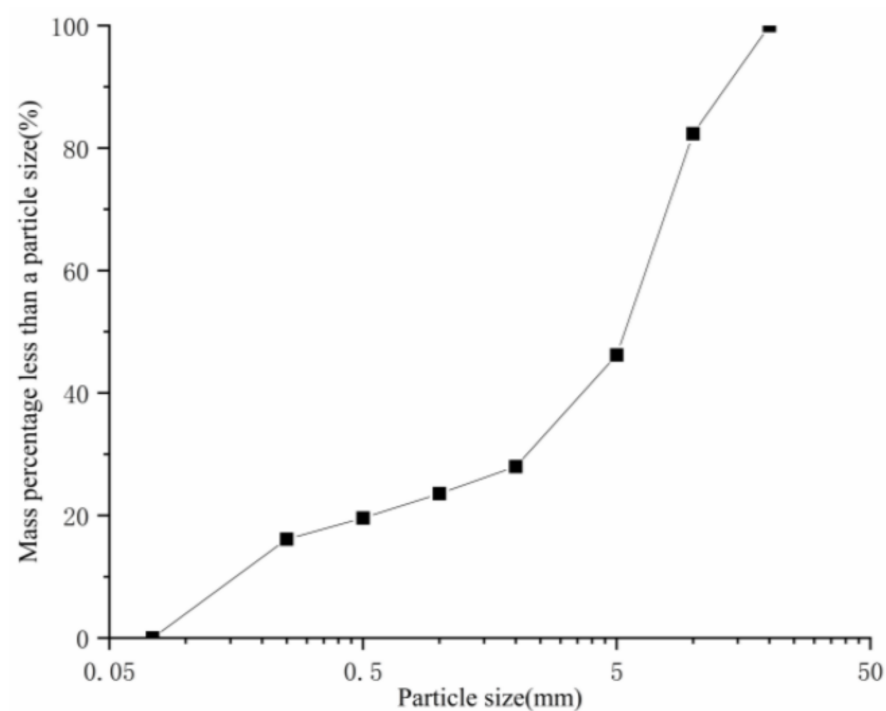


Figure 1. Rain size distribution curve.

Table 1. Soil physical parameters.

Natural Moisture Content (%)	Proportion	Liquid Limit (%)	Plastic Limit (%)	Plasticity Index	Maximum Dry Density (g·cm ⁻³)	Optimum Moisture Content (%)
12	2.63	21.5	29	7.5	1.96	12.4

Table 2. Soluble salt ion content (g·kg⁻¹).

Ion	CO ₃ ²⁻	HCO ₃ ⁻	Cl ⁻	SO ₄ ²⁻	Ca ²⁺	Mg ²⁺	K ⁺	Na ⁺
Content	0.032	0.159	2.144	2.607	0.602	0.342	0.012	3.100

2.2. Fly Ash Properties

The first-grade fly ash produced by the fly ash factory in the Yilan district of Harbin, China, was selected as the material for improvement. The contents of elements were determined by an X-ray fluorescence spectrometer (BTX III Benchtop XRD Analyzer, Olympus, Beijing, China) and semi-quantitative detection and analysis method. The test results were based on the relationship between elements and oxides, and the content of oxides was determined. The active ingredients and specific content are shown in Table 3.

Table 3. Performance index of fly ash.

Composition	SiO ₂	Al ₂ O ₃	Fe ₂ O ₃	CaO	MgO	SO ₃	K ₂ O	Na ₂ O	Ignition Loss
Content (%)	45.1	24.2	0.85	0.85	1.58	2.1	3.68	1.06	4.7

3. Test Scheme Design

3.1. Fly Ash Mix Ratio Design

Existing studies have shown that soil strength can be improved by adding 10%–20% fly ash to the soil [18,21,22]. In order to further compare the improvement effect of 10%, 15%, and 20% fly ash content on the strength of saline soil, the improved test scheme is shown in Table 4.

Table 4. Design scheme of the improved material content ratio.

Type	Design Ideas	Content (%)
Without fly ash	—	0
With fly ash	The incorporation of fly ash increased from 10% to 20%	10
		15
		20

3.2. Sample Preparation

The collected natural saline soil was dried and passed through a 2 mm sieve. The fly ash was passed through the same sieve before use. According to the soil samples collected in the early exploration phase, the average natural moisture content of the soil samples was 12.1% based on laboratory tests. In order to make the test conditions closer to the actual working conditions and make the test data more comparable, the water content was controlled at 12.1% in the test process. The dry density of soil samples measured by the compaction test is shown in Table 5.

The fly ash and salted soil were mixed according to the ratio relationship, and distilled water was added according to the mass volume relationship so that the moisture content reached 12.1%. After curing the configured soil sample under standard conditions for 24 h, a hydraulic press was used to press the soil sample into a standard triaxial specimen [23] with a diameter of 39.1 mm and a height of 80 mm in accordance with 95% compaction [23], and the unconfined compression specimen [23] had a diameter of 50 mm and a height

of 50 mm. The specimen was wrapped in plastic film, sealed in a bag, cured in a humid environment for 24 h, and then placed inside a cryogenic box.

Table 5. Physical property index of the sample.

Fly Ash Content (%)	Moisture Content (%)	Wet Density (g·cm ⁻³)	Dry Density (g·cm ⁻³)
0	12.1	2.1524	1.9201
10	12.1	2.1525	1.9202
15	12.1	2.1522	1.9201
20	12.1	2.1529	1.9205

According to the statistical data of the China Weather Network and the local meteorological bureau, the local winter is from October to March of the following year. The average daytime temperature in winter is -4.3 °C and the average night temperature is -13.9 °C, and thus -13.9 °C was selected as the freezing test temperature. The samples were frozen in a cryogenic chamber at -13.9 °C for 6 h and then melted in a cryogenic chamber at 20 °C for 6 h.

3.3. Unconfined Compression Test

The unconfined compressive test was carried out at room temperature (20 °C) following the Test Rules for Stabilized Materials of Highway Engineering Inorganic Binding Materials (JTG E51-2009). The cylindrical soil samples ($\Phi 50$ mm \times 50 mm) were compared using a microcomputer-controlled electronic testing machine (WDW-50, Changchun Kexin Test Instrument Co., Ltd., Changchun, China). During the test, the deformation rate was 1 mm/min, and the loading data and displacement were automatically recorded by the data recording instrument to calculate the corresponding stress and strain and draw the stress-strain curve.

3.4. Triaxial Test

Considering practical engineering, due to the rapid construction speed, the water and air in the soil pores are not completely eliminated. In order to better simulate the actual working conditions and at the same time avoid the negative effect of the triaxial consolidation test on the original soil structure, the use of an automatic triaxial apparatus (TSZ-6, Nanjing NingXi soil instrument factory, Nanjing, China) for cylindrical soil samples ($\phi 39.1$ mm \times 80 mm) was not consolidated in an undrained triaxial compression test to obtain the shear strength. In order to reduce the disturbance to the soil during the process of placing the sample, the sample was placed in the triaxial apparatus after the frozen component of the last freeze-thaw cycle was completed and thawing had occurred for 6 h. In order to ensure the consistency of the thawing process and reduce the influence of the ambient temperature on the test data, the ambient temperature of the triaxial instrument was set to 20 °C during the thawing test. The confining pressures applied to the soil samples were set at 100, 200, 300, and 400 kPa, and the shear strain rate was 0.8 mm/min. When there was no obvious failure in the test specimens, the principal stress difference at a strain of 15% was adopted as the failure value, and the temperature remained unchanged during the test. Based on triaxial test data, the cohesion and internal friction angle of the soil samples were obtained using the Mohr-Coulomb criterion.

3.5. SEM Test

SEM was used to observe the surface microstructure of the soil samples, and the microstructure of the soil samples was quantitatively analyzed by image processing software. In the experiment, SEM (Apreo 2 SEM, Thermo Scientific, Suzhou, China) was used to observe the soil samples under different freeze and thaw cycles. In order to prevent disturbance of the soil structure, the dried pieces were peeled off along the crack, and soil samples with relatively flat surfaces were selected for cutting to ensure that the length and

width of the samples after cutting were 10 mm. The cut sample was fixed on a conductive copper sheet and placed in a 105 °C oven for drying for 48 h. The dry samples were sprayed with gold to ensure good electrical conductivity. The soil samples were then observed by SEM.

3.6. Acquisition of Microscopic Parameters

In this study, IPP software was used to process the micrographs of soil samples under different conditions to obtain microscopic pore parameters. To reduce the data differences caused by human factors during image processing and data extraction, the same processing method was used for each soil sample photo. The processing steps of the SEM photos were as follows: image conversion and cropping, brightness and contrast adjustment, image morphology processing and binarization processing, and image parameter processing. To ensure that the calculation results of different photos were comparable, the first three steps of image processing were processed by the same Matlab calculation code. In the process of obtaining microscopic parameters, the selection of the image magnification factor and the setting of the threshold have an important influence on the image processing results under SEM [10]. Magnification refers to the conclusions of existing studies [10,24,25]. Magnification was combined with the characteristics of the soil used in the test to ensure that the microstructures and pore changes of the samples were relatively clearly reflected in the photos taken. Finally, a micrograph with a magnification of 500 times was selected for analysis. The same image was observed, results with poor observation effects were discarded, and the average was taken as the final threshold of image binarization. IPP software can be used to obtain the basic micropore parameters, including the perimeter, area, and diameter and to select the parameters required by the test to characterize the micropore of the sample. The specific meaning and calculation method of each parameter follow.

- Porosity

Since the total pore area extracted from the SEM image is a concept on the plane, the porosity obtained is the porosity on the two-dimensional plane. Porosity is expressed as the percentage pore area relative to the total size of the SEM image. The specific expression is as follows:

$$N = \frac{S_0}{S} \times 100 \quad (1)$$

where S_0 represents the total pore area, and S represents the total area of the microscopic image. Porosity can reflect the pore content of the sample under certain circumstances.

- Average pore diameter

The average pore diameter of each pore in the SEM image can be directly calculated using IPP software. For a single pore, the average pore diameter refers to the arithmetic average of each line segment's length connecting the two points of the outer contour of the measured object and passing through the center of the mass. For the samples being tested, the average pore diameter of all pores was calculated as the average pore diameter of the sample \bar{D} .

- Surface fluctuation fractal dimension

The fractal dimension reflects the spatial effectiveness occupied by a complex form, and it is a measure of the irregularity of a complex form. At present, a large number of studies have shown that the soil fractal structure can be used to characterize soil pores, and the microstructure of soil can be studied based on fractal theory [26,27]. The fractal dimension of pore surface fluctuation is generally expressed by F , which can vividly reflect the morphological characteristics, arrangement characteristics, and particle size distribution characteristics of soil particles to a certain extent. The specific expression is as follows:

$$F = -\lim_{\varepsilon \rightarrow 0} \frac{\ln N(\varepsilon)}{\ln \varepsilon} \quad (2)$$

where ε is the length of the grid in image segmentation, and $N(\varepsilon)$ is the response to the total number of grid microstructure pictures.

4. Results and Discussion

4.1. Unconfined Compressive Strength Characteristics

4.1.1. Stress-Strain Curve

The pressure-strain curves of the samples with four fly ash contents were obtained through unconfined compressive strength tests, as shown in Figure 2. It can be seen from the figure that all samples with fly ash were under strain-softening, with the curves being convex and having a peak value. The loading process of the test could be roughly divided into several stages. The sample was in the particle compaction stage in the early stage, which is axial compression, with smaller pores and a smaller curve slope. Then, the soil sample was in the elastic deformation stage; the curve was linear, and the gradient increased. The slope of the line in this stage was equal to the elastic modulus. When the strain increased, the volume of the soil samples expanded under compression, and cracks appeared on the surface. Finally, the curve showed a downward trend, and the crack of the sample expanded rapidly until it was destroyed. This curve fully reflects the process of deformation and failure of the sample. An increase in the fly ash content will increase the unconfined compressive strength of the soil. With the increase in the fly ash content, the unconfined compressive strength of the soil first increased and then decreased. When the fly ash content was 15%, the maximum compressive strength of the soil was obtained.

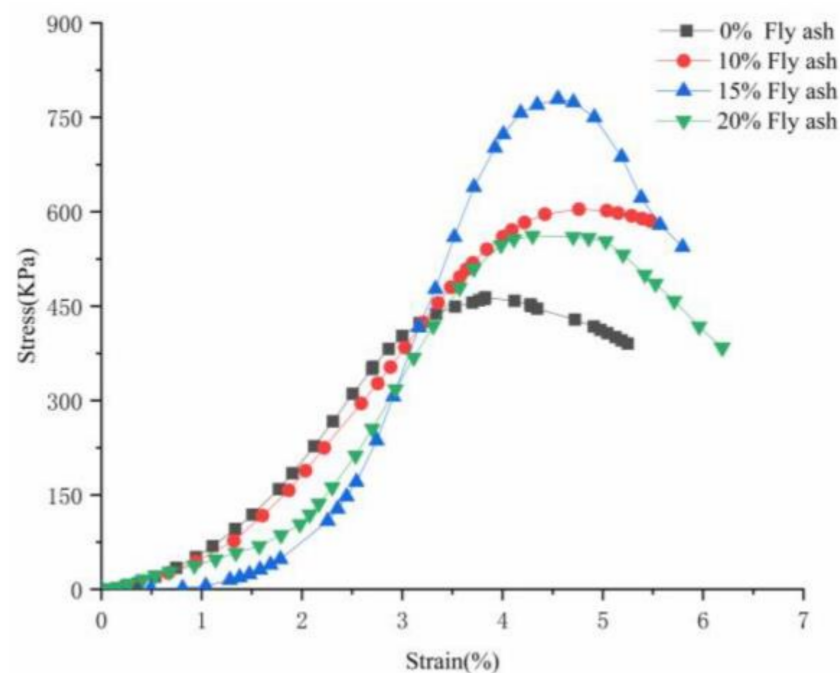


Figure 2. Stress-strain curve.

4.1.2. Relationship between the Unconfined Compressive Strength, Number of Freeze-Thaw Cycles, and the Fly Ash Content

According to the stress-strain curves of the salinized soil samples obtained from the test, the peak value of each curve was taken as the unconfined compressive strength value of the samples, and the unconfined compressive strength of samples with different fly ash contents and different freeze-thaw cycles was obtained, as shown in Figure 3. As can be seen from the image, with a certain fly ash content, the specimen's unconfined compressive strength decreased continuously with the increase in the number of freeze-thaw cycles. According to the relationship between the number of freeze-thaw cycles and the unconfined compressive strength of samples, within the range of freeze-thaw processes set by the test,

when the fly ash content was given, the unconfined compressive strength of samples was inversely correlated with the number of freeze-thaw cycles, which can be expressed as

$$q_u = A \cdot N^B \quad (11 \geq N \geq 1) \quad (3)$$

where q_u represents the unconfined compressive strength of the sample; N is the number of freeze-thaw cycles, and $11 \geq N \geq 1$; A and B are fitting parameters.

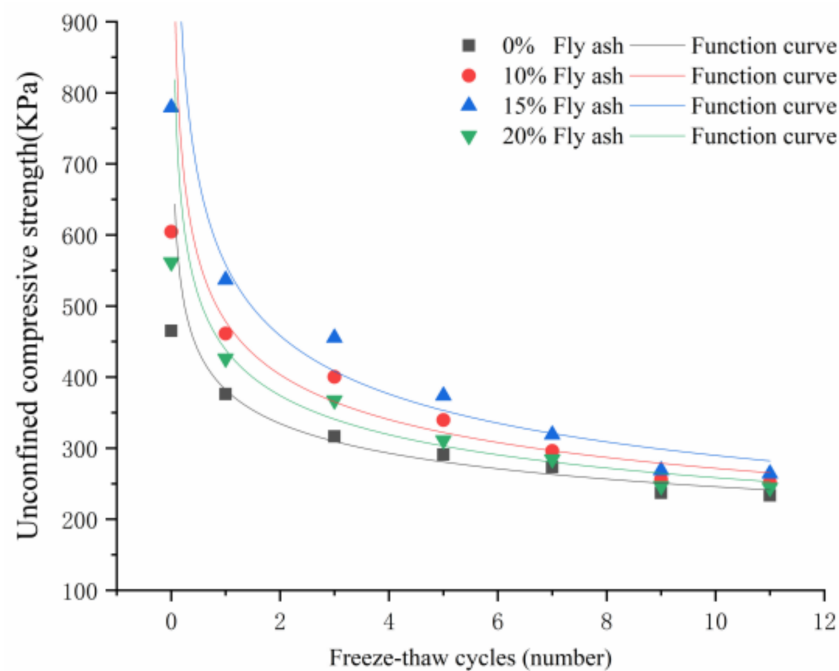


Figure 3. Relationship between the number of freeze-thaw cycles and unconfined compressive strength.

Figure 4 shows that adding fly ash can improve the unconfined compressive strength of saline soil; under the condition of a certain number of freeze-thaw cycles, the unconfined compressive strength of salinized soil showed a trend of first increasing and then decreasing with an increase in the fly ash content. When the amount of fly ash mixed was 15%, the unconfined compressive strength of the saline soil was the highest. It can be seen from Table 6 that when the number of freeze-thaw cycles was less than seven, the unconfined compressive strength decreased significantly with the increase in the number of freeze-thaw cycles, and the unconfined compressive strength decreased significantly when the freeze-thaw cycle number was one. When the number of freeze-thaw cycles exceeds seven, the unconfined compressive strength attenuation rate of the sample slowed down. After 11 cycles of freezing and thawing, the saline soil strength with different fly ash contents decreased under different situations. The strength of the decrease of saline soil with 0%, 10%, 15%, and 20% fly ash contents was 49.8%, 58.41%, 66.11%, and 56.49%, respectively. With the increase in the fly ash content, the strength decrease first increased and then decreased. When the fly ash content was 15%, the strength decrease was the largest after the freeze-thaw cycle. The unconfined compressive strength of salinized soil with fly ash after different freeze-thaw cycles was greater than that of salinized soil with fly ash. It can be seen that the content of fly ash has a strong influence on the unconfined compressive strength of saline soil under freeze-thaw cycles.

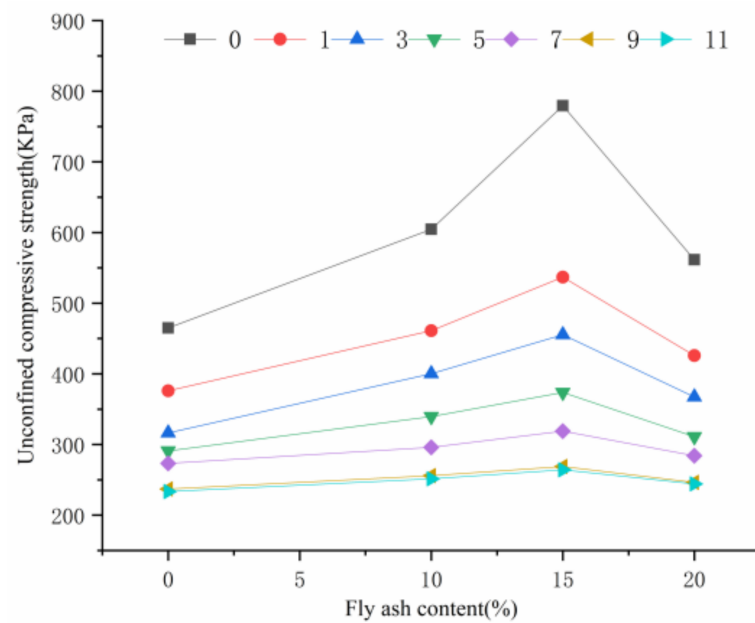


Figure 4. Relationship between the fly ash content and unconfined compressive strength.

Table 6. The unconfined compressive strength of the samples.

Fly Ash Content (%)	Unconfined Compressive Strength of Specimens with Different Freeze-Thaw Cycles (KPa)							(%)
	0	1	3	5	7	9	11	
0	464.96	376.05	316.36	290.84	273.31	236.94	233.37	49.80
10	604.58	461.08	400.29	339.49	296.05	255.84	251.43	58.41
15	779.36	536.81	455.28	373.75	318.91	268.78	264.07	66.11
20	561.52	425.97	367.30	311.08	284.23	246.35	244.27	56.49

4.1.3. Parameter Analysis and Verification

The fitting parameter A can represent the foundation strength fitted inversely, and the relationship curve between it and the fly ash content of the sample is shown in Figure 5. Based on the relationship curve between parameter A and the fly ash content, it can be seen that parameter A and the fly ash content showed a linear change. With the increase in the fly ash content of the sample, parameter A showed a linear increase and then A decreased linearly. The inflection point occurred at a fly ash content of 15%. In other words, with the increase in the fly ash content in salinized soil, the unconfined compressive strength of the sample first increased and then decreased. The reason is that the addition of fly ash will change the original grading of salinized soil [28]; the smaller particle size of fly ash can change the initial pore structure of salinized soil, and the cement formed by fly ash hydration will flocculate small soil particles into large ones [26]. Therefore, the addition of fly ash will affect the uniaxial compressive strength of salinized soil samples. The relationship between fitting parameter A and the fly ash content can be expressed as:

$$\begin{cases} A = 11.61X + 380.11 & R^2 = 0.9965 \quad (0 \leq X \leq 15) \\ A = -23.942X + 917.35 & R^2 = 1 \quad (15 < X \leq 20) \end{cases} \quad (4)$$

where X represents the content of fly ash in salinized soil, and the correlation coefficient $R^2 > 0.99$ proves that this formula has a good fitting property.

The fitting parameter B represents the strong attenuation of saline soil with different fly ash contents after the action of the freeze-thaw cycle. The variation curve of the fitting parameter B with the fly ash content is shown in Figure 6. With the increase in the fly ash

content, parameter B generally presents a linear trend of an initial decrease and then an increase, which is specifically expressed as follows:

$$\begin{cases} B = -0.00623X - 0.19216 & R^2 = 0.99942 \quad (0 \leq X \leq 15) \\ B = 0.01102X - 0.45002 & R^2 = 1 \quad (15 < X \leq 20) \end{cases} \quad (5)$$

where X represents the content of fly ash in salinized soil, and the correlation coefficient $R^2 > 0.99$ proves that this formula has a good fitting property.

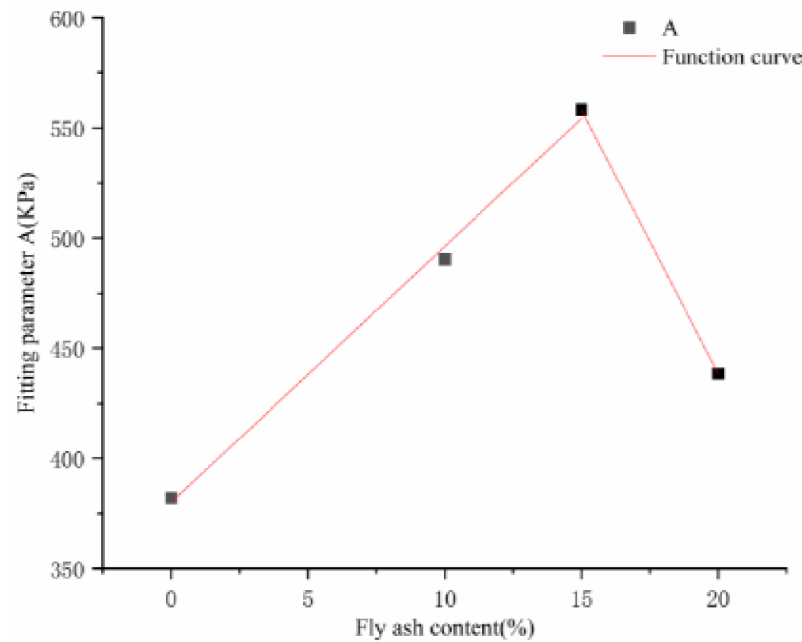


Figure 5. Relationship between parameter A and fly ash content.

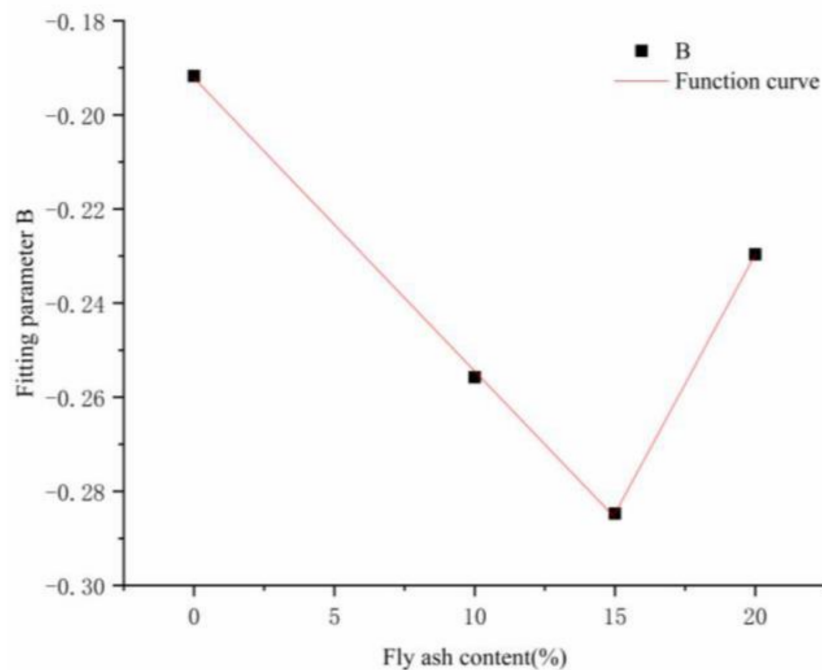


Figure 6. Relationship between parameter B and fly ash content.

The experimental data of the unconfined compressive strength of saline soil with seven freeze-thaw cycles were used to calculate the strength loss formula. The specific verification results are shown in Table 7. The calculated values of the unconfined compressive strength of saline soil with different fly ash contents after the freeze-thaw cycle were basically consistent with the experimental values. This indicates that the strength loss calculation formula reflects the variation in unconfined compressive strength with the number of freeze-thaw cycles when the fly ash content is given in the test. As the number of freeze-thaw cycles increases and the fly ash content increases, further tests will be required to verify the reliability of the formula.

Table 7. Comparison of test strength and computed strength for different fly ash content after seven freeze-thaw cycles.

Fly Ash Content (%)	Test Strength (KPa)	Computed Strength (KPa)	Error (%)
0	273.31	261.53	4.31
10	296.05	302.43	2.16
15	318.91	317.95	0.30
20	284.23	281.79	0.85

4.2. Analysis of Triaxial Shear Data

4.2.1. Shear Strength Analysis

Taking triaxial shear data of samples without freeze-thaw cycles under a confining pressure of 100 kPa as an example, the relationship between the principal stress difference and axial strain of saline soil with different fly ash contents was analyzed, as shown in Figure 7. The results show that, under the given initial test conditions, the principal stress of the differential-axial strain curve of salinized soil with different fly ash contents showed a strain-hardening law, consistent with the shear test characteristics of silty clay [29]. The peak stress obtained from the test data is the shear strength. The addition of fly ash can improve the shear strength of salinized soil. With the increase in the fly ash content, the shear strength of salinized soil first increased and then decreased, which is consistent with the result obtained from the unconfined compressive strength test.

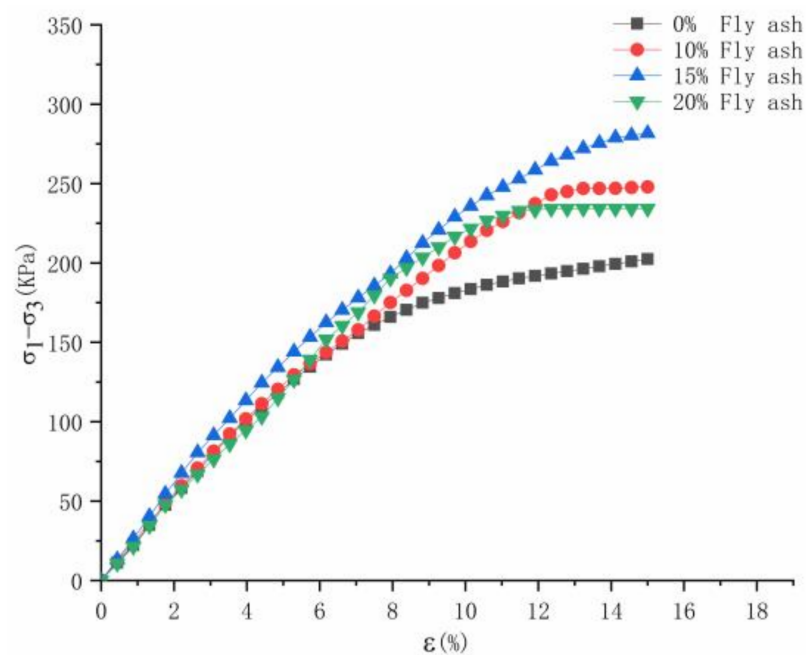


Figure 7. Principal stress difference-axial stress relationship.

In order to better respond to saline soil shear strength in the process of freezing and thawing circulation losses, according to Li et al. [24], the shear strength loss ratio is

$$\lambda = \frac{Q_0 - Q(n)}{Q_0} \times 100\% \quad (6)$$

where Q_0 presents the shear strength of the sample without freeze-thaw cycles, $Q(n)$ represents the shear strength of the sample after freeze-thaw cycles, and n represents the number of freeze-thaw cycles.

Figure 8 shows the relationship between the shear strength loss rate of salinized soil and the number of freeze-thaw cycles when the fly ash content is 0%, 10%, 15%, and 20%. As can be seen from the figures, the shear strength loss rate of salinized soil with different fly ash contents gradually increased with the increase in the number of freeze-thaw cycles, and the strength degradation phenomenon of salinized soil became increasingly obvious. The evolution of the peak strength loss rate under different confining pressures was roughly the same. When the specimen was under constant confining pressure and there were fewer than seven freezing and thawing cycles, with an increase in freeze-thaw cycles, the shear strength loss rate increased rapidly. When there were more than seven freeze-thaw cycles, the circulation loss rate of shear strength was affected, which shows that with the increase in freeze-thaw cycles, the effects of these cycles on saline soil strength decreased. When the fly ash content was constant, with the increase in confining pressure on the sample, the shear strength of saline soil increased, and the loss rate of peak strength decreased, which is similar to the research conclusion of Li et al. [24] for loess.

4.2.2. Influence of Freeze-Thaw Cycles on the Shear Strength Parameters of the Soil

According to the Moors-Coulomb theory, the cohesion and internal friction angle values of saline soil with different fly ash contents after different freeze-thaw cycles can be calculated, as shown in Figures 9 and 10. Figure 9 shows the relationship curve between the cohesion and the number of freeze-thaw cycles. It can be seen that the cohesion of soil samples with different fly ash contents decreased gradually at first and then tended to stabilize in the process of the freeze-thaw cycles. After one and three freeze-thaw cycles, the soil cohesion decreased greatly and tended to stabilize when the number of freeze-thaw cycles reached seven. After three freeze-thaw cycles, the cohesion of the soil decreased the most, and the cohesion of soil with 0%, 10%, 15%, and 20% fly ash decreased by 8.05%, 10.56%, 10.82%, and 10.48%, respectively. During one to three freeze-thaw cycles, the decrease in the cohesion of soil mixed with fly ash was greater than that of plain soil. After seven freeze-thaw cycles, the change in the cohesion of soil mixed with fly ash was more stable than that of plain soil. Figure 10 shows the relationship curve between the internal friction angle and the number of freeze-thaw cycles. It can be seen that under the action of freeze-thaw cycles, the internal friction angle will change with the change in the number of freeze-thaw cycles. For salinized soil with different fly ash contents, when the number of freeze-thaw cycles ranged from zero to seven, the internal friction angle decreased rapidly with the increase in the number of freeze-thaw cycles. After seven freeze-thaw cycles, the internal friction angle decreased slowly, and the change tended to stabilize. This is because in the process of the freeze-thaw cycles, the water in saline soil undergoes a phase change due to the change in temperature, and the expansion of the water crystal volume squeezes the soil skeleton and changes the original structure of the soil skeleton. During the freeze-thaw cycle, the sulfate in salinized soil also expands its crystalline volume. Studies have proved that the first freeze-thaw cycle leads to a large expansion of the water volume, and the crystallization of sodium sulfate also significantly increases the volume of salt [3,30]. During the freeze-thaw cycle, there is a temperature difference between the inside and outside of saline soil; when the sample is placed in a low-temperature environment, a temperature gradient is generated between the surface and center. According to the water transfer theory, if the temperature is not below freezing, the center of the sample does not freeze, and water is transferred to

the surface, with water-soluble sodium sulfate transferred to the sample surface. During thawing at room temperature, when the surface temperature is higher than the center, and the temperature gradient is opposite to that of the frozen sample, the water and salt on the surface of the saline soil is transferred to the center of the sample. The migration force caused by the migration of water and salt in the freeze-thaw process also affects the internal structure of the sample, weakening the binding force between soil particles, leading to the decrease of cohesion and the change in the internal friction angle. With the increase in the number of freeze-thaw cycles, soil particles gradually form a new stable structure, which changes the contact point and contact mode between particles. The influence of freeze-thaw cycles on the binding force and internal friction angle gradually decreases. After seven freeze-thaw cycles, the soil particles are rearranged, and the structure tends to become stable.

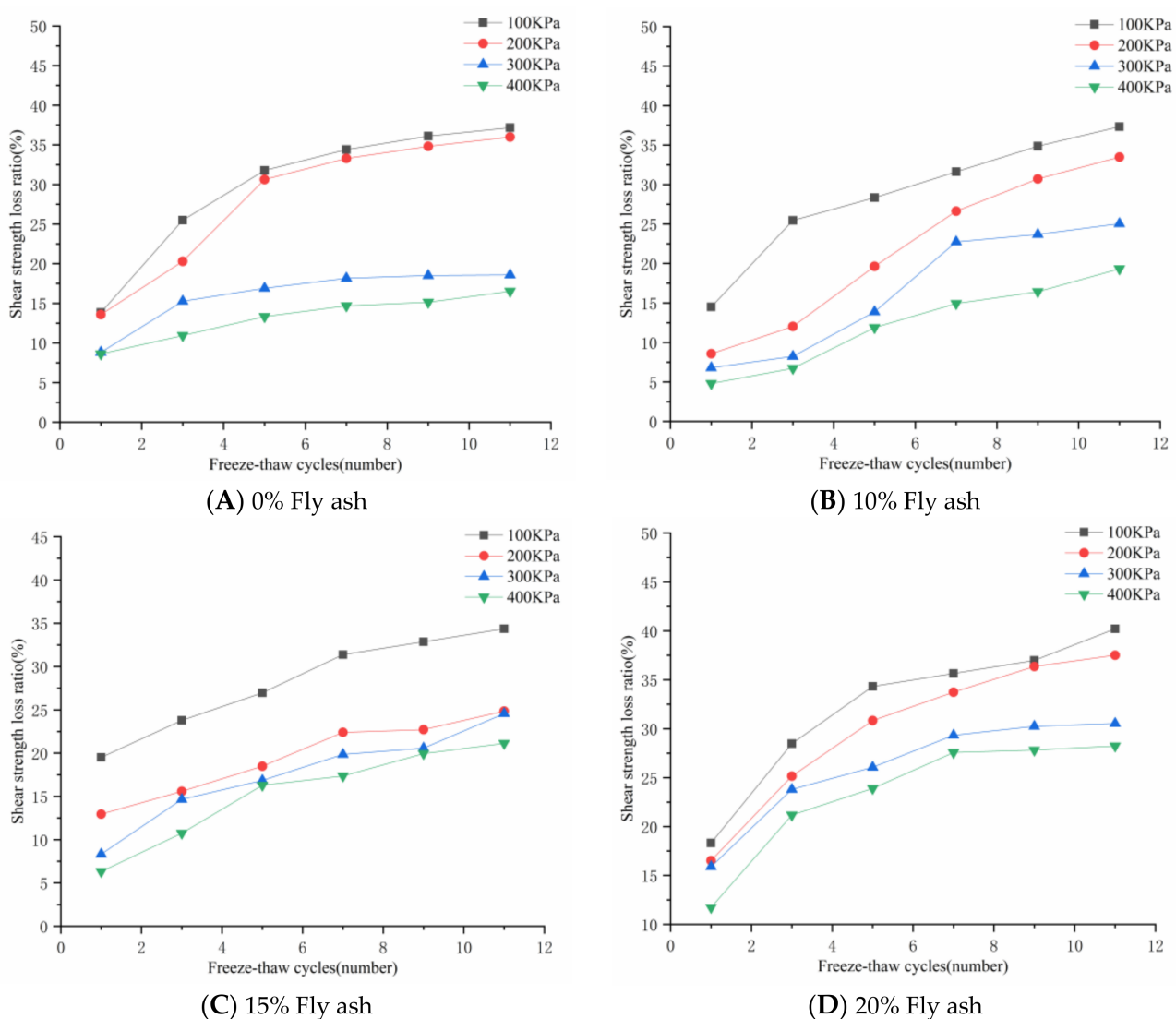


Figure 8. Influence curve of number of freeze-thaw cycles on unconfined compressive strength.

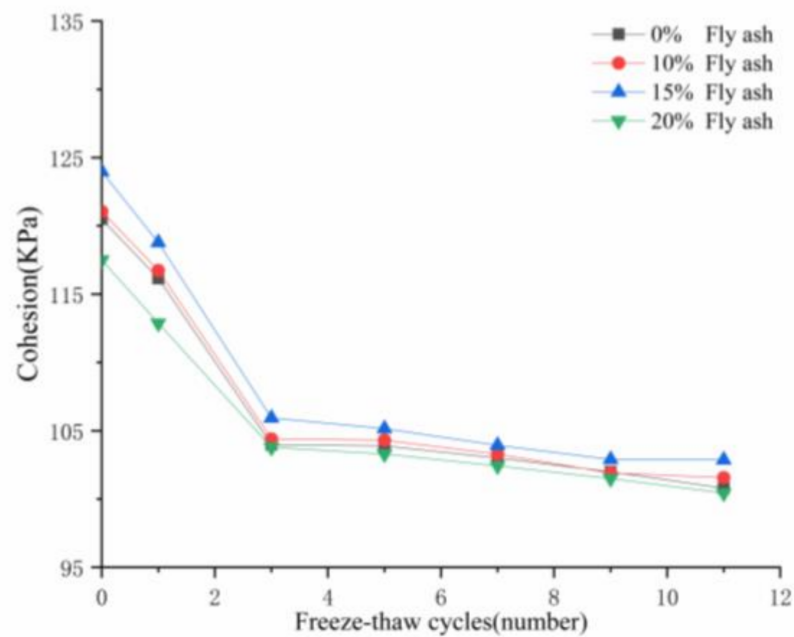


Figure 9. Cohesion-freeze-thaw cycle curve.

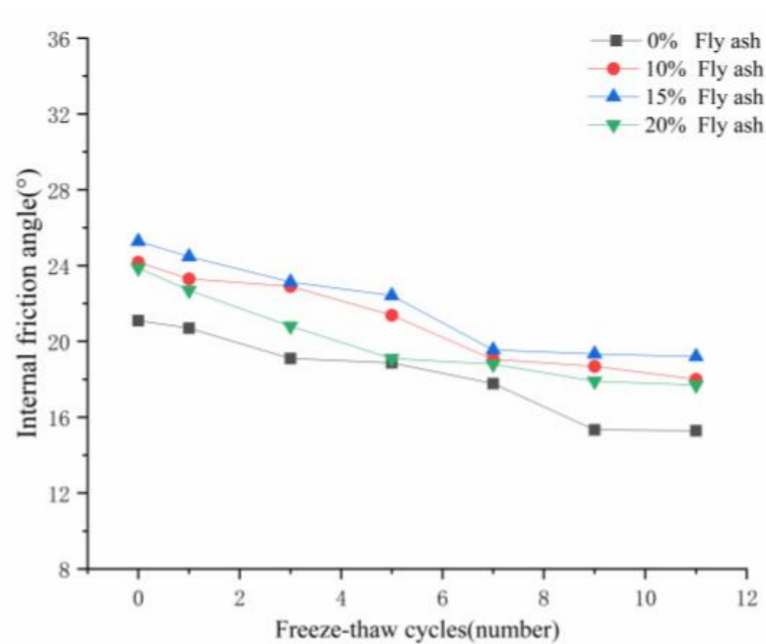


Figure 10. Internal friction angle-freeze-thaw cycle relation curve.

To better describe the variation in the internal friction angle of soil samples undergoing successive freeze-thaw cycles, the attenuation ratio of the internal friction angle was defined because the variation of the internal friction angle of soil samples undergoing successive freeze-thaw cycles was not obvious compared with the change in cohesion α_{n-m} :

$$\alpha_{n-m} = \frac{C_n - C_m}{C_n} \times 100\% \quad (7)$$

where C_n is the internal friction angle of soil after n freeze-thaw cycles, C_m is the internal friction angle of soil after m freeze-thaw cycles, and $n > m$. The specific attenuation ratio of the internal friction angle of soil is shown in Table 8. During one to seven freeze-thaw cycles, the attenuation of the internal friction angle of soil was large. After seven freeze-

thaw cycles, the attenuation of the internal friction angle was small, and the change tended to stabilize. This is similar to the variation trend of shear strength and the cohesion of soil with the change in the number of freeze-thaw cycles. Although the α_{5-3} value of the L1 group was lower than that of α_{3-1} and α_{9-7} of the L1 group, combined with the analysis of the change in the attenuation ratio of the internal friction angle of each group, the data did not affect the overall change, and the possibility of such a phenomenon caused by experimental error and human factors could not be ruled out. With the addition of 0%, 10%, 15%, and 20% fly ash to the saline soil, α_{11-1} was 27.54%, 25.56%, 24.05%, and 25.85%, respectively. The internal friction angle of soil mixed with fly ash was superior to that of plain soil, and with the increase in the dosage of fly ash, the attenuation ratio of the internal friction angle decreased first and then increased. When 15% fly ash was added, the attenuation of the internal friction angle of soil was the lowest.

Table 8. Attenuation ratio of the internal friction angle of soil samples.

Number	Fly Ash Content (%)	α_{10}	α_{31}	α_{5-3}	α_{7-5}	α_{9-7}	α_{11-9}
L1	0	4.90%	7.73%	1.20%	5.78%	4.72%	0.33%
L2	10	3.64%	6.72%	6.64%	10.90%	1.89%	0.69%
L3	15	3.20%	5.48%	3.07%	12.80%	1.07%	0.72%
L4	20	4.90%	8.37%	8.17%	5.57%	4.79%	1.12%

4.2.3. Influence of the Fly Ash Content on the Shear Strength Parameters of the Soil

Figure 11 shows the relationship between cohesion and the fly ash content. In the case of each vertical pressure and a certain number of freeze-thaw cycles, the cohesion of salted soil with less than 15% fly ash improved to a certain extent. When the fly ash content exceeded 15%, soil cohesion decreased and was slightly lower than that of salted soil with 10% fly ash. When 15% fly ash was added to the saline soil, the soil cohesion reached the maximum. The variation trend of the cohesion of salted soil with fly ash was basically consistent with that of the soil shear strength with fly ash, which explains, to some extent, the phenomenon that the shear strength of soil increased first and then decreased with the increase in the fly ash content in salted soil. As can be seen from the relationship curve in Figure 12, the internal friction angle of the soil shear strength index first increased and then decreased with the increase in the fly ash content. When the fly ash content increased from 0% to 10%, the increase in the internal friction angle was less than that when the fly ash content increased from 10% to 15%. When the fly ash content increased to 20%, the soil cohesion showed a downward trend. This still occurred when the number of freeze-thaw cycles experienced by the soil varied. The variation trend was more obvious when the soil was subjected to fewer than six freeze-thaw cycles. This is because fly ash is composed of fine powdery particles. In general, the particle size of fly ash ranges from 10 μm to 90 μm [31,32], which is much smaller than that of soil particles, so it has a good filling effect on the internal structure of saline soil. Hydrolysis and hydration reactions can occur in a certain environment. Ion exchange reduces the dispersion of soil particles and compacts the soil. The agglomeration can reduce the dispersion of soil particles and plays a skeletal role in the soil structure. Fly ash is mainly composed of SiO_2 , Al_2O_3 , Fe_2O_3 , Na_2O , K_2O , and CaO [33,34]. After incorporation into salinized soil, Na_2O and K_2O dissolve rapidly under the action of water in the soil to generate K^+ , Na^+ , and OH^- . CaO dissolves to generate $\text{Ca}(\text{OH})_2$ and $\text{Mg}(\text{OH})_2$ to react and generate divalent calcium, magnesium, and hydroxide ions. The adsorption of divalent calcium and magnesium ions by soil particles results in an ion exchange reaction, which reduces the dispersion of salinized soil particles and makes it easy for soil to form stably. CaCO_3 and MgCO_3 formed by the reaction not only have high strength and are insoluble in water but can also increase the bond between soil particles [22,34]. However, the gel formed by the action of calcium silicate, calcium ferrite, and calcium aluminate hardens in the water environment, and the soil particles form a network connection on the basis of the original structure, which improves the strength of the soil. Within a specific scope, increasing the amount

of mixed fly ash has a good effect in improving the saline soil strength; when the fly ash mixture ratio reaches an absolute value, a continued increase in the dosage of fly ash will greatly change the original components of the saline soil, and the influence of the physical and mechanical properties of fly ash on soil improvement becomes increasingly obvious. The addition of fly ash exceeding the threshold value may lead to a decline in soil strength.

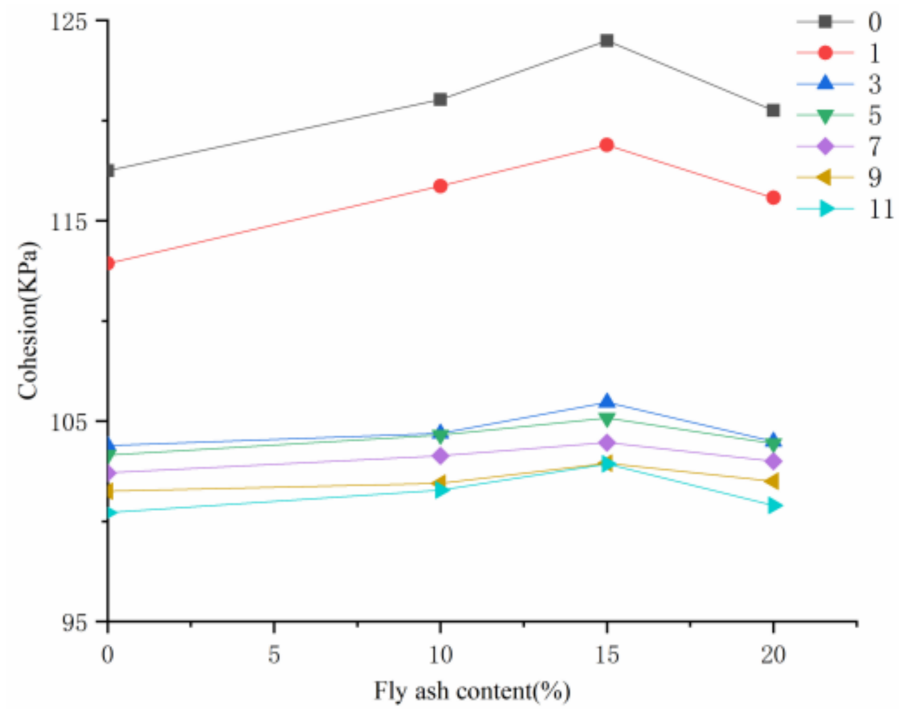


Figure 11. Cohesion-fly ash content relationship curve.

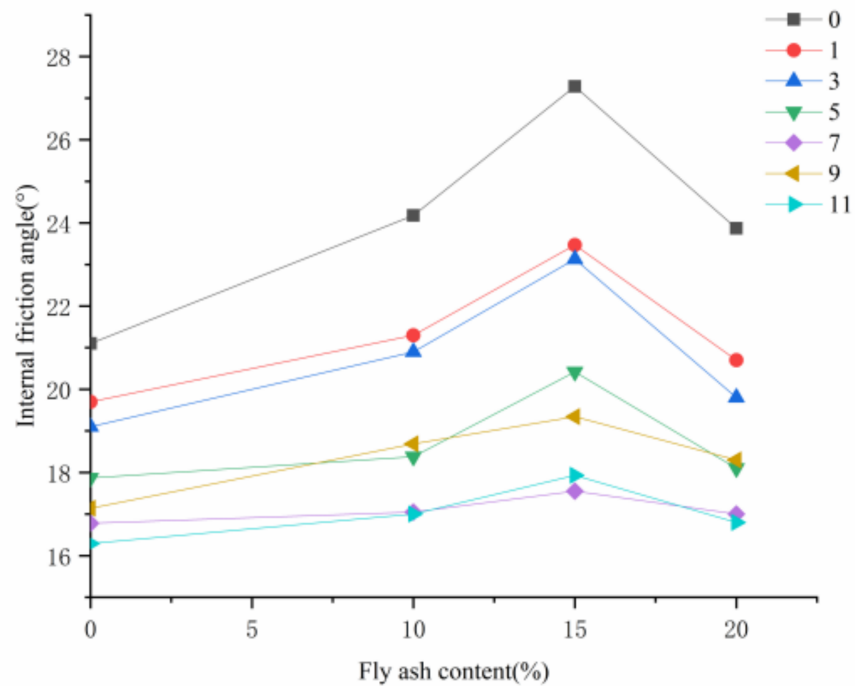


Figure 12. Internal friction angle and fly ash content curve.

4.3. Microstructural Characteristics

4.3.1. Microstructure Overview of the Saline Soil Samples

Figure 13 shows some micrographs of salinized soil samples with different fly ash contents and freeze-thaw cycles obtained through SEM tests. In order to better show the influence of fly ash on the microstructure of salinized soil, salinized soil with fly ash contents of 0% and 15% was selected for analysis. The vertical direction in Figure 13 shows the surface microstructure of saline soil after different freeze-thaw cycles with the same fly ash content. With the increase in freeze-thaw cycles, cracks and pores appeared on the soil sample surface, and the surface structure gradually changed from a flocculation structure to an agglomeration structure. As can be seen from Figure 13, the sample surface without freeze-thaw cycles was relatively flat and compact, with a complete structure. After one freeze-thaw cycle, cracks and pores appeared on the surface of the soil sample, the structure became loose, and the soil particles were broken. With the increase in freeze-thaw cycles, pore and fissure development occurred on the surface of the soil sample; when there were one to seven freeze-thaw cycles, fractures and pore development occurred rapidly. In addition, the distance between the soil particles increased, leading to a weakened connection between the soil particles and reduced saline soil strength, and cohesion decreased rapidly because the connection between the soil particles and the soil skeleton structure changed, and the internal friction angle was affected. After seven freeze-thaw cycles, the distribution of pores and cracks in saline soil tended to stabilize, the pore content of the soil slightly increased, and the structural change was not obvious. The new microstructure gradually formed, and the changes in the strength, cohesion, and internal friction angle of the saline soil tended to stabilize.

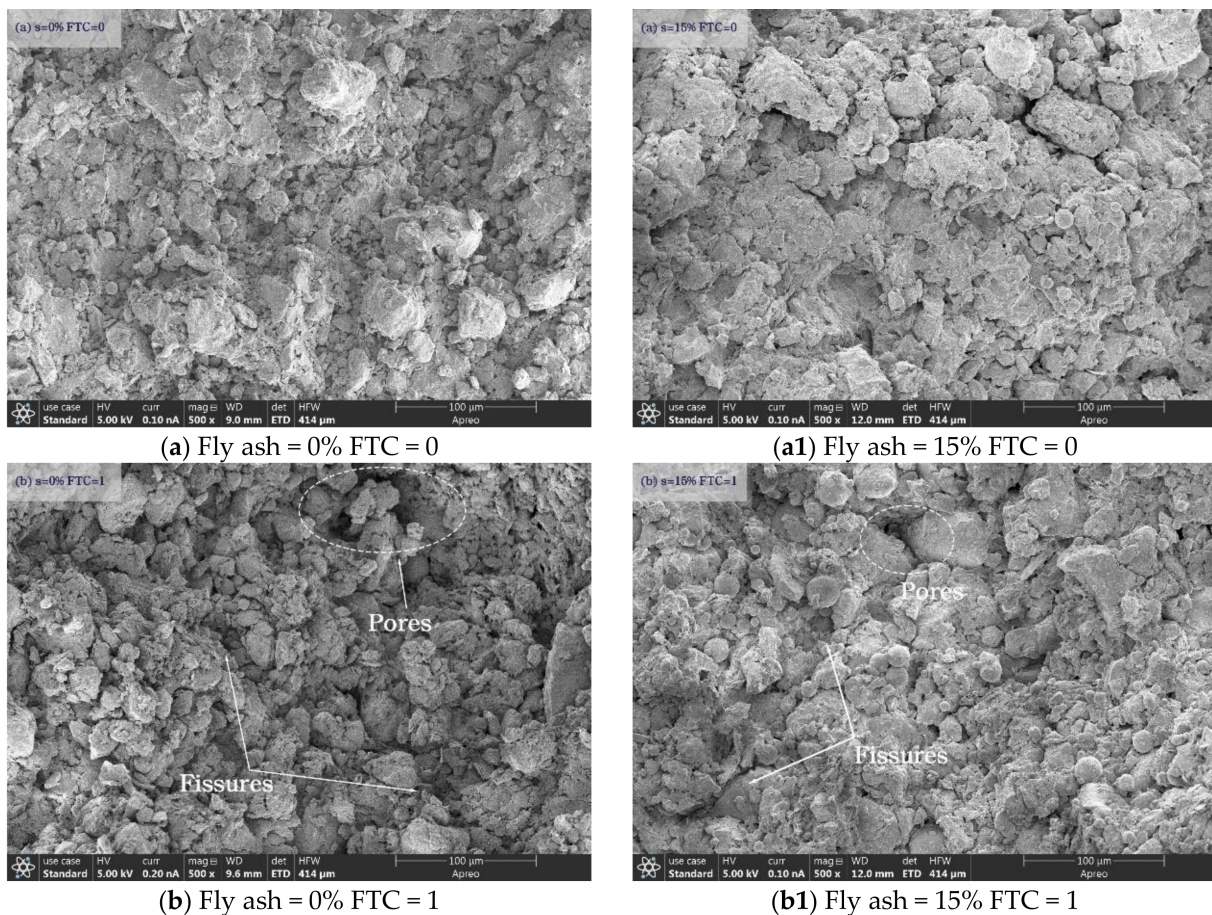


Figure 13. Cont.

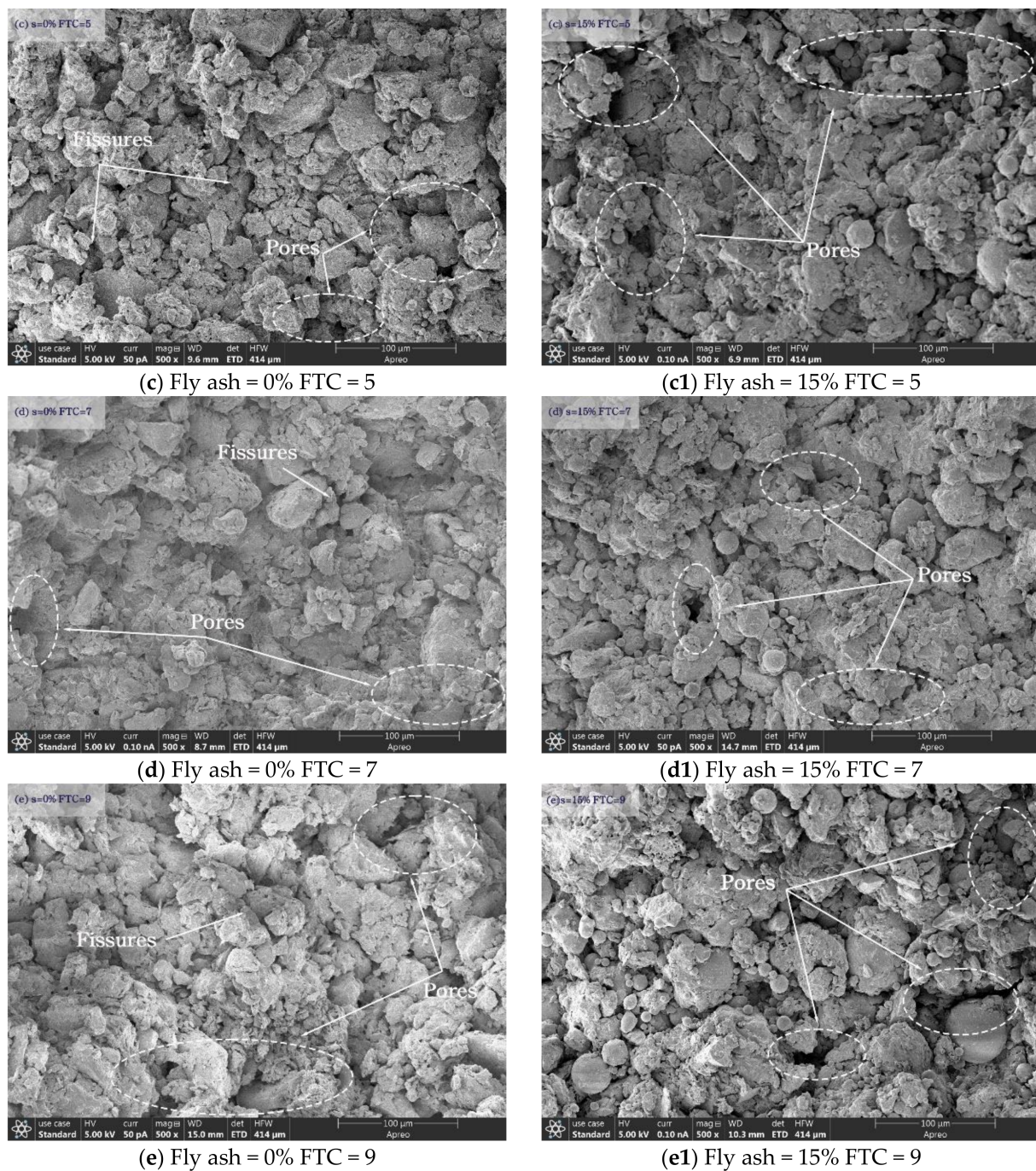


Figure 13. Micrographs of soil samples under different fly ash contents and freeze–thaw cycles.

By comparing the microstructure of the plain soil and the salinized soil with 15% fly ash in Figure 13 after the freeze–thaw cycle, it was found that the salinized soil with fly ash had a denser structure and relatively fewer pores. After the same number of freeze–thaw cycles, there were significantly fewer pores and cracks than in the salinized soil without fly ash. In the process of the freeze–thaw cycle, the development speed of the cracks and pores in the saline soil mixed with fly ash was slower, and the agglomeration phenomenon was more obvious. Figures 14 and 15 show the microstructure of the salinized soil without fly ash and that with 15% fly ash, respectively. After fly ash was added, the flake structure was significantly reduced, and the agglomeration effect of the particles was obvious at a 1000 times ratio compared with that without improved materials. The improved material and the corresponding components in the soil exhibited physical and chemical interactions,

and the condensate generated by the reaction produces calcium sulfate, calcium carbonate, and other substances, which have good water stability and are difficult to dissolve in water. These substances can enhance the connection between soil particles and can improve the strength of saline soil.

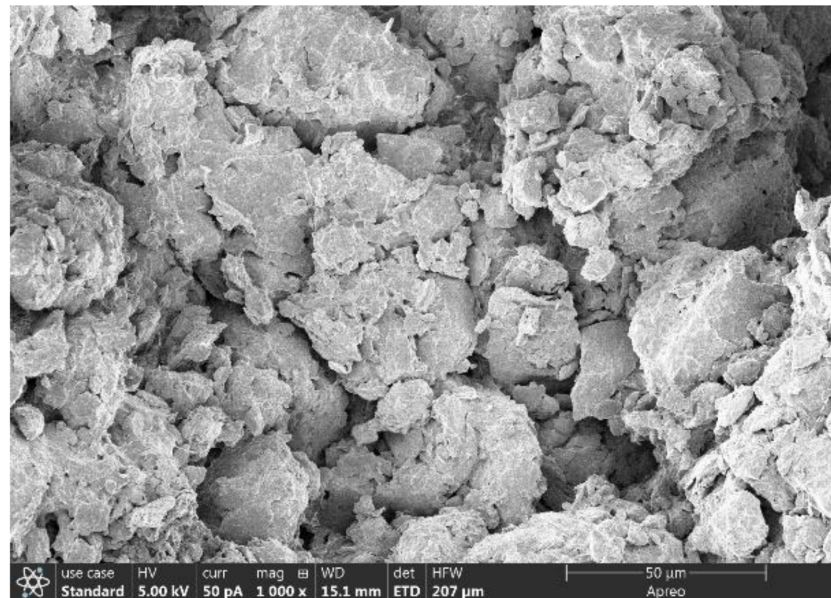


Figure 14. Microstructure of saline soil.

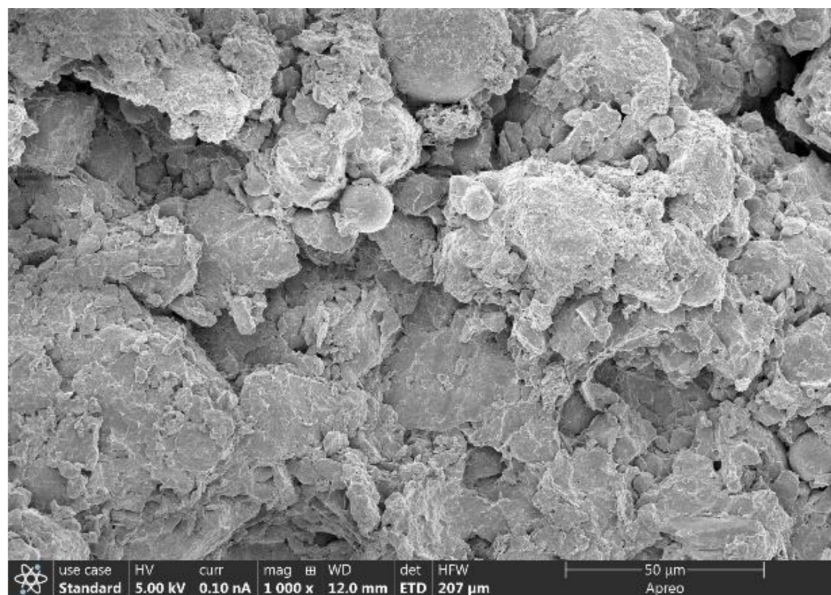


Figure 15. Microstructure of modified saline soil (fly ash = 15% FTC = 1).

4.3.2. Porosity

Figure 16 shows the variation in the porosity of salinized soil with 0% and 15% fly ash contents with the number of freeze-thaw cycles. It can be seen that the porosity of saline soil mixed with fly ash and without fly ash increased with the increase in the number of freeze-thaw cycles. The salinized soil porosity with 15% coal ash was significantly lower than that without fly ash, and the increase in the porosity of the salinized soil with fly ash was lower than that without fly ash upon going through the same number of freeze-thaw cycles. When the number of freeze-thaw cycles was between one and seven, the increase in the

porosity of the samples of the two types of saline soil was high. When the number of freeze-thaw cycles exceeded seven, the increase in the porosity of the saline soil slowed. With the increasing number of freeze-thaw cycles, the change in soil structure tended to be slow. After a certain number of freeze-thaw cycles, the soil structure will reach a new balance [35]. By comparing Figures 3, 8C and 16, it can be found that porosity was negatively correlated with the soil sample strength on the whole, and the growth rate of porosity was positively correlated with the decay rate of the soil strength. The higher the porosity of the soil, the lower the soil strength, and the faster the porosity development rate, the faster the soil strength decay rate, which is similar to the existing research conclusions [36]. The addition of fly ash can change the grain distribution of soil, fill the pores to a certain extent, reduce the soil porosity, and improve soil strength. Therefore, the strength of the salinized soil with fly ash is still better than that of the salinized soil without fly ash under the same conditions after freeze-thaw cycles.

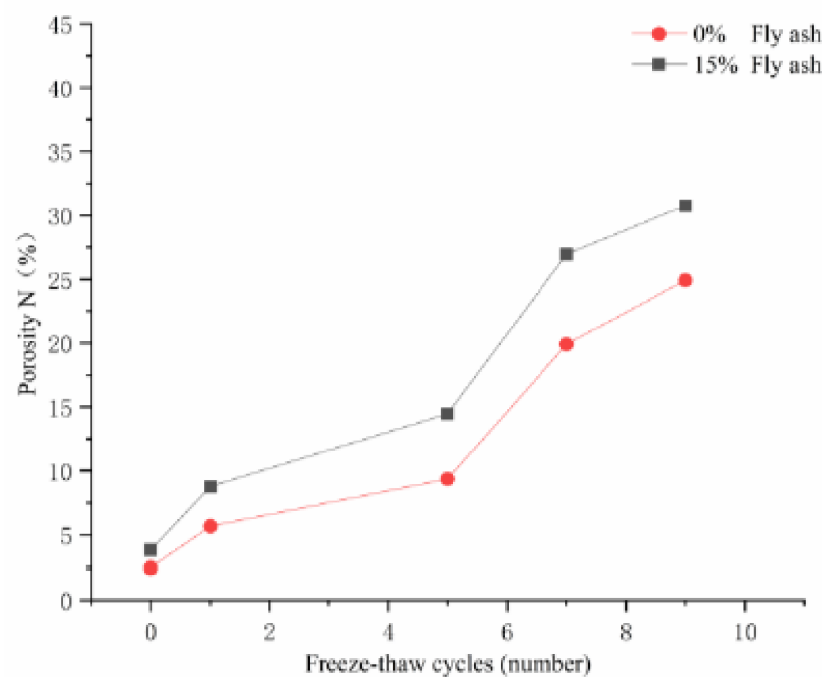


Figure 16. Porosity-freeze-thaw cycles curve.

4.3.3. Average Pore Diameter

Figure 17 shows the variation curve of the average pore diameter of salinized soil with a fly ash content of 0% or 15% under freeze-thaw cycles. It can be seen that under the conditions of different fly ash contents, the variation trend of the average pore size of the soil sample under the freeze-thaw cycle was similar to that of the porosity. With the increase in the number of freeze-thaw cycles, the average pore size of the soil samples showed an increasing trend in general. The increase rate of the average pore size in the process of one to seven freeze-thaw cycles was higher than that in the soil samples after seven freeze-thaw cycles. During the freeze-thaw cycle, the soil skeleton and internal soil particles' position changes, and the average pore diameter also changes [7]. When the soil structure reaches a new equilibrium, the internal soil tends to be stable, and the change in the average pore diameter also slows down. The influential mechanism of the effect of fly ash addition on the average pore size is similar to that described in the previous section. That is to say, the filling effect of fly ash changed the average pore size of the soil [37] and also had a certain influence on the variation in the average pore size of the soil in the freeze-thaw cycle.

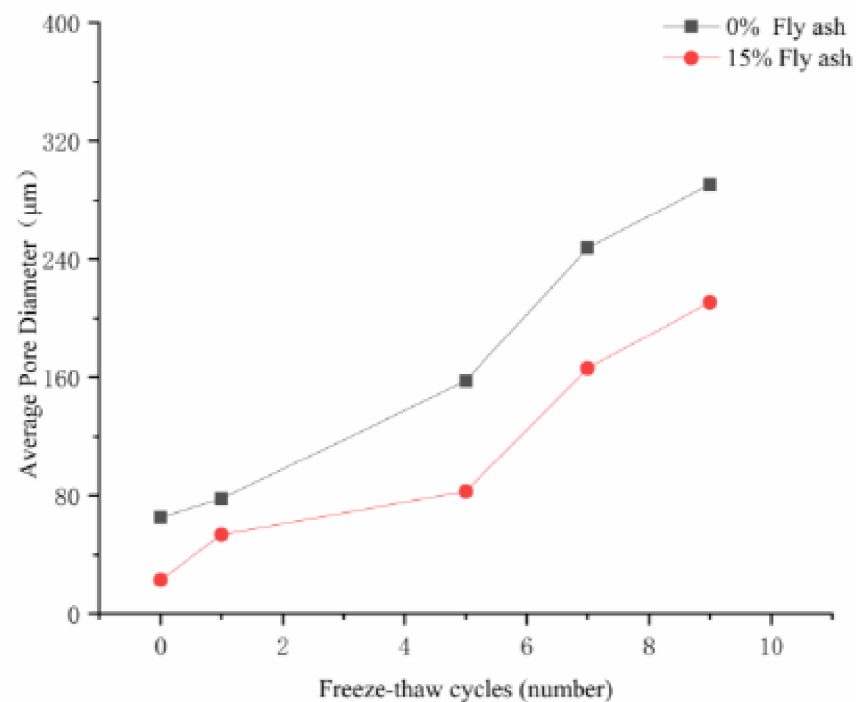


Figure 17. Average Pore Diameter-freeze-thaw cycles curve.

4.3.4. Surface Fluctuation Fractal Dimension

Figure 18 shows the change in the fractal dimension of surface fluctuation with 0% and 15% fly ash content under freeze-thaw cycles. It can be seen that, with the increase in the number of freeze-thaw cycles, the saline soil's surface fractal dimension with different fly ash contents fluctuated between 1.8 and 1.9, showing a change that first increased and then decreased. Overall, the change was small, and the regularity was not obvious. In general, with the increase in the number of freeze-thaw cycles, the fractal dimension of surface undulation showed a downward trend, and the fractal dimension of the surface undulation of saline-soil mixed with fly ash showed a downward trend. This saline soil showed that the pore contour complexity and roughness changed with the change in the number of freeze-thaw cycles and were generally reduced by the freeze-thaw cycles, which is consistent with existing research conclusions [10].

However, the addition of fly ash can reduce the complexity and roughness of the pore profile of saline soil. The variation trend of the internal friction angle of saline soil was consistent with the variation in the fractal dimension of surface fluctuation, as the internal friction angle was closely related to soil particles and pore shape. The change in the pore morphology during the test had a certain influence on the internal friction angle of the soil.

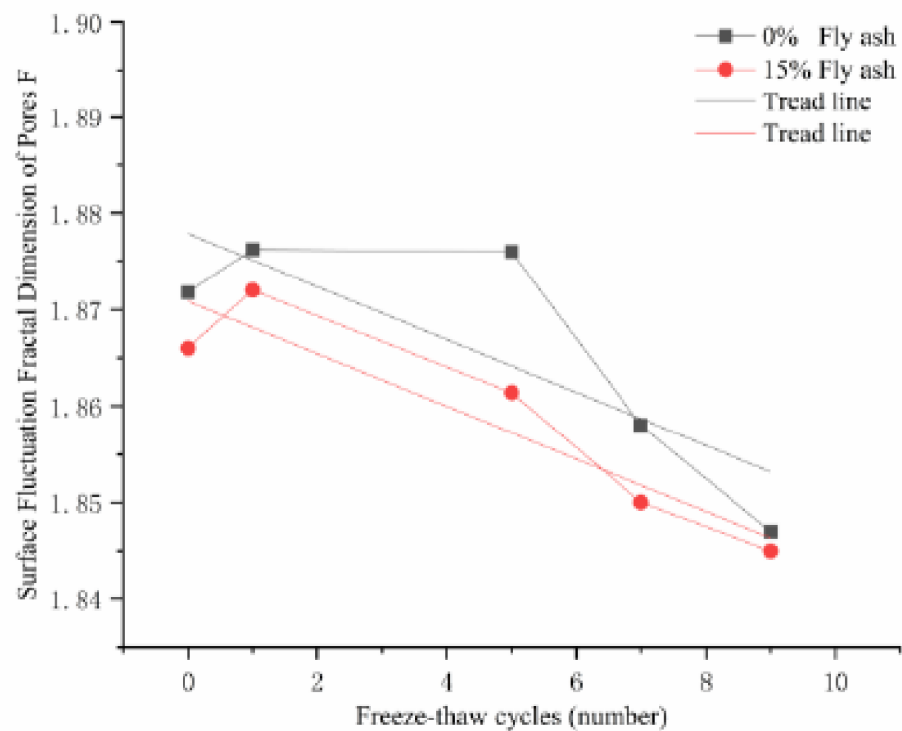


Figure 18. Surface fluctuation fractal dimension of pore freeze-thaw cycles.

5. Conclusions

In this paper, through an unconfined compressive test, triaxial test, and SEM test, the strength, strength parameters, and microstructural changes of saline soil from the Suihua-Daqing expressway area with different fly ash contents under freeze-thaw cycle conditions were qualitatively and quantitatively analyzed. In addition, the modification mechanism and improvement effect of this type of saline soil with fly ash were studied. The conclusions are as follows:

- Saline soil with different fly ash contents was subjected to strain softening. The unconfined compressive strength of salinized soil could be improved by adding fly ash, with the strength increasing first and then decreasing with the increase in fly ash content. The unconfined compressive strength of salinized soil with fly ash was better than that of salinized soil without fly ash after different freeze-thaw cycles.
- The freeze-thaw cycle leads to a decrease in the strength of saline soil. The strength loss was relatively large before seven freeze-thaw cycles. When the number of freeze-thaw cycles was more than seven, the strength decline rate of the salinized soil slowed down and tended to stabilize gradually. With the increase in the number of freeze-thaw cycles, the cohesion and internal friction angle of the improved salinized soil showed a general trend of decreasing first and then tending to stabilize.
- According to the SEM test results, the surface of the unfreeze-thaw soil sample was more flat and the structure was more compact than that of the freeze-thaw soil sample. With the increase in the number of freeze-thaw cycles, the proportion of pores and cracks in the soil sample increased, the average pore diameter increased, the structure tended to become loose, and the complexity of pores and surface roughness decreased slightly. According to the qualitative analysis of the microstructure, the soil sample strength was negatively correlated with porosity and average pore size in general.
- The advantages of fly ash in saline soil are as follows: (1) The compactness of soil can be improved through the pore filling effect, and the porosity and average pore diameter of soil can be significantly reduced. (2) The chemical reaction products obtained by adding fly ash reduce probably the dispersion of soil particles, and

CaCO₃ and MgCO₃, which have gelling effects, improve probably the connectivity between soil particles, thus improving the strength of the soil particles.

- Through testing and analysis, the shear strength, cohesion, and internal friction angle of soil with 15% fly ash content obtained the highest values.

Author Contributions: Conceptualization, Z.C. and G.C.; methodology, G.C.; software, Z.Y.; validation, Z.C., Z.G. and H.G.; formal analysis, D.Z.; investigation, Z.C.; resources, Z.C.; data curation, Z.C.; writing—original draft preparation, G.C.; writing—review and editing, Z.C.; visualization, Z.C.; supervision, G.C.; project administration, G.C. and C.X. All authors have read and agreed to the published version of the manuscript.

Funding: This work was supported by the Undergraduate Innovation and Entrepreneurship Training Program (202010225018); National Natural Science Foundation of China (No. 50538030); Natural Science Foundation of Heilongjiang Province (E201149), and the Fundamental Research Funds for the Central Universities (DL12CB03).

Institutional Review Board Statement: Not applicable.

Informed Consent Statement: Not applicable.

Data Availability Statement: All data analyzed in this study is presented in Tables in the text, or was obtained from publicly accessible databases mentioned in the text.

Acknowledgments: All support is gratefully acknowledged.

Conflicts of Interest: The authors declare no conflict of interest.

References

1. Wang, J.; Wang, Q.; Kong, Y.; Han, Y.; Cheng, S. Analysis of the pore structure characteristics of freeze-thawed saline soil with different salinities based on mercury intrusion porosimetry. *Environ. Earth Sci.* **2020**, *79*, 1–16. [\[CrossRef\]](#)
2. Han, Y.; Wang, Q.; Kong, Y.; Cheng, S.; Wang, J.; Zhang, X.; Wang, N. Experiments on the initial freezing point of dispersive saline soil. *Catena* **2018**, *171*, 681–690. [\[CrossRef\]](#)
3. Bing, H.; He, P. Experimental investigations on the influence of cyclical freezing and thawing on physical and mechanical properties of saline soil. *Environ. Earth Sci.* **2011**, *64*, 431–436. [\[CrossRef\]](#)
4. An, L.; Yang, B.; Yan, F.; Wang, Z. Study on durability reliability sensitivity of transmission tower foundation in saline soil. *Chin. J. Appl. Mech.* **2016**, *33*, 459–465. [\[CrossRef\]](#)
5. Yıldız, M.; Soğancı, A. Effect of freezing and thawing on strength and permeability of lime-stabilized clays. *Sci. Iran.* **2012**, *19*, 1013–1017. [\[CrossRef\]](#)
6. Eskişar, T.; Altun, S.; Kalıpcılar, I. Assessment of strength development and freeze–thaw performance of cement treated clays at different water contents. *Cold Reg. Sci. Technol.* **2015**, *111*, 50–59. [\[CrossRef\]](#)
7. Han, Y.; Wang, Q.; Wang, N.; Wang, J.; Zhang, X.; Cheng, S.; Kong, Y. Effect of freeze-thaw cycles on shear strength of saline soil. *Cold Reg. Sci. Technol.* **2018**, *154*, 42–53. [\[CrossRef\]](#)
8. Zhang, W.; Ma, J.; Tang, L. Experimental study on shear strength characteristics of sulfate saline soil in Ningxia region under long-term freeze-thaw cycles. *Cold Reg. Sci. Technol.* **2019**, *160*, 48–57. [\[CrossRef\]](#)
9. Xu, J.; Li, Y.; Lan, W.; Wang, S. Shear strength and damage mechanism of saline intact loess after freeze-thaw cycling. *Cold Reg. Sci. Technol.* **2019**, *164*, 102779. [\[CrossRef\]](#)
10. Wang, J.; Wang, Q.; Lin, S.; Han, Y.; Cheng, S.; Wang, N. Relationship between the Shear Strength and Microscopic Pore Parameters of Saline Soil with Different Freeze-Thaw Cycles and Salinities. *Symmetry* **2020**, *12*, 1709. [\[CrossRef\]](#)
11. Liu, Y.; Wang, Q.; Liu, S.; ShangGuan, Y.; Fu, H.; Ma, B.; Chen, H.; Yuan, X. Experimental investigation of the geotechnical properties and microstructure of lime-stabilized saline soils under freeze-thaw cycling. *Cold Reg. Sci. Technol.* **2019**, *161*, 32–42. [\[CrossRef\]](#)
12. Viran, P.A.G.; Binal, A. Effects of repeated freeze–thaw cycles on physico-mechanical properties of cohesive soils. *Arab. J. Geosci.* **2018**, *11*, 250. [\[CrossRef\]](#)
13. Wang, S.; Ding, J.; Xu, J.; Ren, J.; Yang, Y. Shear Strength Behavior of Coarse-Grained Saline Soils after Freeze-Thaw. *KSCE J. Civ. Eng.* **2019**, *23*, 2437–2452. [\[CrossRef\]](#)
14. Aldaood, A.; Bouasker, M.; Al-Mukhtar, M. Impact of freeze–thaw cycles on mechanical behaviour of lime stabilized gypseous soils. *Cold Reg. Sci. Technol.* **2014**, *99*, 38–45. [\[CrossRef\]](#)
15. Qi, J.; Zhang, J.; Zhu, Y.J. Influence of freezing-thawing on soil structure and its soil mechanics significance. *Chin. J. Rock Mech. Eng.* **2003**, *22*, 2690–2694.
16. Kamei, T.; Ahmed, A.; Shibi, T. Effect of freeze–thaw cycles on durability and strength of very soft clay soil stabilised with recycled Bassanite. *Cold Reg. Sci. Technol.* **2012**, *82*, 124–129. [\[CrossRef\]](#)

17. Lv, Q.; Jiang, L.; Ma, B.; Zhao, B.; Huo, Z. A study on the effect of the salt content on the solidification of sulfate saline soil solidified with an alkali-activated geopolymer. *Constr. Build. Mater.* **2018**, *176*, 68–74. [[CrossRef](#)]
18. Li, H.; Shen, H.; Shen, J. Shearing strength and durability of hypersaline soil solidified with fly ash. *J. Lanzhou Univ. Technol.* **2015**, *140*–144. [[CrossRef](#)]
19. Chinese Standard. GB/50021-2001. Ministry of Construction, Code for Geotechnical Engineering Investigation. Available online: <http://www.mohurd.gov.cn> (accessed on 25 January 2021).
20. Chinese Standard. JTG/E40-2007. Highway Geotechnical Test Procedures. Available online: <http://zs.mot.gov.cn/mot/s> (accessed on 25 January 2021).
21. Wang, J.; Wang, Q.; Wang, P.; Zhong, X. Effect of adding amount of fly ash on dynamic constitutive relationship of modified loess. *Chin. J. Geotech. Eng.* **2013**, *35*, 156–160.
22. Zhang, S.; Yang, X.; Xie, S.; Yin, P. Experimental study on improving the engineering properties of coarse grain sulphate saline soils with inorganic materials. *Cold Reg. Sci. Technol.* **2020**, *170*, 102909. [[CrossRef](#)]
23. Chinese Standard. JTGD30-2015. Specification for Highway Subgrade Design. Available online: <http://zs.mot.gov.cn/mot/s> (accessed on 25 January 2021).
24. Li, Z.; Yang, G.; Liu, H. The Influence of Regional Freeze–Thaw Cycles on Loess Landslides: Analysis of Strength Deterioration of Loess with Changes in Pore Structure. *Water* **2020**, *12*, 3047. [[CrossRef](#)]
25. Moretti, L.; Conficconi, M.; Natali, S.; D’Andrea, A. Statistical analyses of SEM-EDS results to predict the quantity of added quicklime in a treated clayey soil. *Constr. Build. Mater.* **2020**, *253*, 118852. [[CrossRef](#)]
26. Chen, H.; Zhang, J.; Yan, H. Quantitative evaluation of microstructure characteristics of cement consolidated soil. *Bull. Int. Assoc. Eng. Geol.* **2013**, *72*, 233–236. [[CrossRef](#)]
27. Ruilin, H.; Guolin, G.; Xiangquan, L.; Lizhong, Z.J. Microstructure effect on the subsidence of loess. *Geology* **1999**, *7*, 161–167.
28. Takhelmayum, G.; Savitha, A.; Krishna, G.S. Laboratory study on soil stabilization using fly ash mixtures. *International Journal of Engineering Science and Innovative Technology* **2013**, *2*, 477–482.
29. Qi, J.; Vermeer, P.A.; Cheng, G. A review of the influence of freeze-thaw cycles on soil geotechnical properties. *Permafr. Periglac. Process.* **2006**, *17*, 245–252. [[CrossRef](#)]
30. Wan, X.; Hu, Q.; Liao, M. Salt crystallization in cold sulfate saline soil. *Cold Reg. Sci. Technol.* **2017**, *137*, 36–47. [[CrossRef](#)]
31. Sarkar, A.; Rano, R.; Mishra, K.; Sinha, I. Particle size distribution profile of some Indian fly ash—A comparative study to assess their possible uses. *Fuel Process. Technol.* **2005**, *86*, 1221–1238. [[CrossRef](#)]
32. Pandey, V.C.; Singh, N. Impact of fly ash incorporation in soil systems. *Agric. Ecosyst. Environ.* **2010**, *136*, 16–27. [[CrossRef](#)]
33. Ahmaruzzaman, M. A review on the utilization of fly ash. *Prog. Energy Combust. Sci.* **2010**, *36*, 327–363. [[CrossRef](#)]
34. Li, M.; Ma, C.; Sun, Z.M.; Yao, X.Y. Mechanical properties distribution of lime-fly ash solidified oil contaminated soil in a coastal environment. *Eur. J. Environ. Civ. Eng.* **2020**, *10*, 1–16. [[CrossRef](#)]
35. Xu, J.; Ren, J.; Wang, Z.; Wang, S.; Yuan, J. Strength behaviors and meso-structural characters of loess after freeze-thaw. *Cold Reg. Sci. Technol.* **2018**, *148*, 104–120. [[CrossRef](#)]
36. Zhang, Y.; Bing, H.; Yang, C. Influences of freeze-thaw cycles on mechanical properties of silty clay based on SEM and MIP test. *Chin. J. Rock Mech. Eng.* **2015**, *34*, 3597–3603.
37. Mir, B.A.; Sridharan, A. Physical and Compaction Behaviour of Clay Soil–Fly Ash Mixtures. *Geotech. Geol. Eng.* **2013**, *31*, 1059–1072. [[CrossRef](#)]